Trajectory Generation on SE(3) with Applications to a Class of Underactuated Vehicles

Conference Paper · December 2017

CITATIONS
0

READS
26

3 authors, including:

Sanyal Amit
Syracuse University
125 PUBLICATIONS **1,471** CITATIONS

SEE PROFILE

2017 IEEE 56th Annual Conference on Decision and Control (CDC)
December 12-15, 2017, Melbourne, Australia

Trajectory Generation on $\mathrm{SE}(3)$ with Applications to a Class of Underactuated Vehicles

Mani H. Dhullipalla, Reza Hamrah, and Amit K. Sanyal[1]

***Abstract*— This paper addresses the problem of generating a continuous and differentiable trajectory on the Lie group of rigid body motions, $\mathrm{SE}(3)$, for a class of underactuated vehicles modeled as rigid bodies. The three rotational degrees of freedom (DOF) are independently actuated, while only one translational DOF is actuated by a body-fixed thrust vector. This model is applicable to a large set of unmanned vehicles, including fixed-wing and rotorcraft unmanned aerial vehicles (UAVs). The formulation utilizes exponential coordinates to express the underactuation constraint as an intrinsic part of the problem. It provides steps to generate a rest-to-rest trajectory after obtaining conditions that guarantee controllability. An attitude trajectory is selected to satisfy the given initial and final attitude state. The position trajectory generation is subsequently posed as an optimal control problem expressed as a linear quadratic regulator (LQR) in the exponential coordinates corresponding to position. As a result, an optimal position trajectory is obtained which ensures that the trajectory generated is feasible with realistic velocities and with given initial pose and final pose, while satisfying the underactuation constraint. Numerical simulation results are obtained that validate this trajectory generation scheme.**

I. Introduction

Autonomous operations of unmanned vehicles are required for several applications where remote human piloting is not feasible or convenient. Increased autonomy is useful in diverse applications like security, agriculture and aquaculture, inspection of civilian infrastructure, space and underwater exploration, wildlife tracking and conservation, package delivery and remote sensing. A critical aspect of safe and reliable operations of unmanned vehicles is that of stable and robust autonomous guidance, navigation and control with onboard hardware. This is particularly true for beyond visual-line-of-sight (BVLOS) operations that require safety and reliability in the presence of obstacles and disturbances like wind. Collision and obstacle avoidance, as well as recovery from external disturbances, may necessitate large maneuvers even if such large maneuvers are not required otherwise. Absence of nonlinear stability in these situations can lead to failure and crash of even remotely piloted vehicles in LOS operations, as shown in this video compilation.

This paper investigates the problem of guiding an underactuated vehicle modeled as a rigid body with four independent control inputs for the six degrees of freedom of translational and rotational motion in three dimensional Euclidean space. The actuators control the three degrees of freedom of rotational motion and provide a body-fixed thrust vector to control the translational motion in a vehicle body-fixed coordinate frame. This actuation model covers a wide range of unmanned vehicles like fixed-wing and rotorcraft unmanned aerial vehicles (UAVs), unmanned underwater vehicles (UUVs), and spacecraft. It is well known that a rigid body with this type of actuation is controllable globally over its state space [1]–[3]. A guidance scheme is then obtained between given waypoints that are prescribed in terms of their poses (positions and orientations). Prior related research on the topics of trajectory generation and tracking of underactuated unmanned vehicles includes [1]–[11].

Trajectory generation schemes for quadrotor UAVs, which satisfy this actuation model, have been treated in the past, for example, in [2], [12], [13]. For large and rapid maneuvers that go beyond hovering or level flight, schemes that can account for large motions are desirable. The trajectory generation scheme given here can generate trajectories requiring large maneuvers in an optimal and stable manner on the Lie group of rigid body motions in three-dimensional Euclidean space, $\mathrm{SE}(3)$. This scheme can then be used in conjunction with robust and stable trajectory tracking control schemes, like those in [14], [15]. Exponential coordinates are used to generate a time trajectory between a given pair of initial pose and final pose on $\mathrm{SE}(3)$, to account for possible large maneuvers required to go between the given pair with a desired degree of differentiability, while avoiding known or detected obstacles. The attitude trajectory between the given initial attitude and final attitude is generated first, because the attitude is fully actuated. This is followed by generating the time trajectory for the position using exponential coordinates. It is noted that the kinematics is linear in the exponential coordinates for the position, which allows representation of the position kinematics as a linear time-varying (LTV) system. Consequently, this position trajectory is then generated in an optimal manner using a linear quadratic regulator (LQR) for this LTV system, such that the unmanned vehicle is regulated to the final desired position.

This paper is organized as follows. Section II introduces the problem of generating a trajectory that complies with the under-actuation constraint. Section III details the steps of the algorithm resulting in the solution that satisfies this constraint. This section also addresses aspects of controllability of the underactuated system, and stable convergence of the generated solution to the desired final pose. Numerical simulation results for the proposed trajectory generation scheme are provided in IV. A summary of analytical and numerical results obtained in this paper and related research directions to be pursued in the near future are provided in

[1]Department of Mechanical and Aerospace Engineering, Syracuse University, Syracuse, NY13244, USA. mdhullip, rhamrah, aksanyal@syr.edu

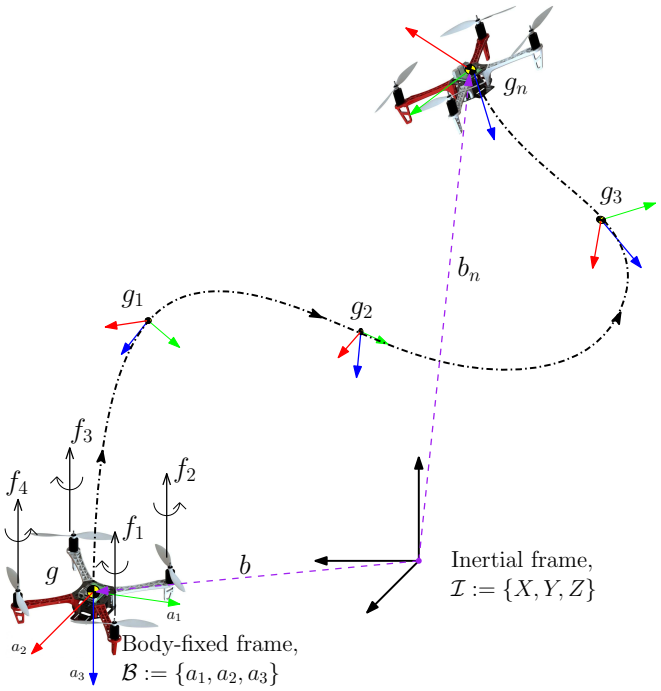

Fig. 1: Trajectory of a UAV between initial and final configurations on SE(3).

section V.

II. Problem Formulation

A. Coordinate frame definition

The configuration of an unmanned vehicle modeled as a rigid body is given by its position and orientation, which are together referred to as its pose. To define the pose of the vehicle, we fix a coordinate frame $\mathcal{B}$ to its body and another coordinate frame $\mathcal{I}$ that is fixed in space and takes the role of an inertial coordinate frame. Let $b \in \mathbb{R}^3$ denote the position vector of the origin of frame $\mathcal{B}$ with respect to frame $\mathcal{I}$, represented in frame $\mathcal{I}$. Let $R \in \mathrm{SO}(3)$ denote the orientation, defined as the rotation matrix from frame $\mathcal{B}$ to frame $\mathcal{I}$. The pose of the vehicle can be represented in matrix form as follows:

$$g = \begin{bmatrix} R & b \\ 0 & 1 \end{bmatrix} \in \mathrm{SE}(3), \tag{1}$$

where $\mathrm{SE}(3) \in \mathbb{R}^{4\times4}$ is the six-dimensional Lie group of rigid body motions (translational and rotational) that is obtained as the semi-direct product of $\mathbb{R}^3$ with $\mathrm{SO}(3)$ [16]. This is also the frame transformation matrix from frame $\mathcal{B}$ to frame $\mathcal{I}$. A conceptual diagram depicting a trajectory on $\mathrm{SE}(3)$ is given in Fig. 1.

Let $\xi \in \mathbb{R}^6$ be the vehicle's velocity vector (with translational velocity $\nu \in \mathbb{R}^3$ and rotational velocity $\Omega \in \mathbb{R}^3$) expressed in coordinate frame $\mathcal{B}$. The vehicle satisfies the kinematics relation

$$\begin{aligned} \dot{g} = g\xi^\vee, \text{where } \xi = \begin{bmatrix} \Omega \\ \nu \end{bmatrix} \in \mathbb{R}^6 \\ \text{and } \xi^\vee = \begin{bmatrix} \Omega^\times & \nu \\ 0 & 0 \end{bmatrix} \in \mathfrak{se}(3) \subset \mathbb{R}^{4\times4}. \end{aligned} \tag{2}$$

Here $(\cdot)^\vee = \{\begin{bmatrix} \Omega^\times & \nu \\ 0 & 0 \end{bmatrix} \in \mathfrak{se}(3) \mid \Omega, \nu \in \mathbb{R}^3\}$, is a vector space isomorphism from $\mathbb{R}^6$ to $\mathfrak{se}(3)$, the associated Lie algebra of $\mathrm{SE}(3)$, and $(\cdot)^\times : \mathbb{R}^3 \to \mathfrak{so}(3) \subset \mathbb{R}^{3\times3}$ is the skew-symmetric cross-product operator that gives the vector space isomorphism between $\mathbb{R}^3$ and $\mathfrak{so}(3)$:

$$x^\times = \begin{bmatrix} x_1 \\ x_2 \\ x_3 \end{bmatrix}^\times = \begin{bmatrix} 0 & -x_3 & x_2 \\ x_3 & 0 & -x_1 \\ -x_2 & x_1 & 0 \end{bmatrix}. \tag{3}$$

B. Kinematics and Inverse Kinematics in Exponential Coordinates

Denote the vector of exponential coordinates in $\mathrm{SE}(3)$ by $X \in \mathbb{R}^6$, which is the concatenation of two vectors $\Theta, \beta \in \mathbb{R}^3$ where Θ characterizes the principal angle and axis of rotation and β is the exponential coordinate corresponding to position. An exponential map (identical to the matrix exponent), as detailed in [17], relates exponential coordinates X to the pose g of the vehicle

$$\begin{aligned} g = \exp(X^\vee), \text{ where } X = \begin{bmatrix} \Theta \\ \beta \end{bmatrix} \in \mathbb{R}^6 \\ \text{and } X^\vee = \begin{bmatrix} \Theta^\times & \beta \\ 0 & 0 \end{bmatrix} \in \mathfrak{se}(3) \subset \mathbb{R}^{4\times4}. \end{aligned} \tag{4}$$

Substituting the expression for pose g into the kinematics relation eq. (2) results in

$$\dot{X} = G(X)\xi, \tag{5}$$

where $G(X)$, as shown in [18], is

$$G(X) = \begin{bmatrix} A(\Theta) & 0 \\ T(\Theta, \beta) & A(\Theta) \end{bmatrix} \tag{6}$$

and

$$\begin{aligned} T(\Theta,\beta) &= \frac{1}{2}(S(\Theta)\beta)^\times A(\Theta) \\ &\quad + \left(\frac{1}{\theta^2} - \frac{1+\cos\theta}{2\theta\sin\theta}\right)(\Theta\beta^{\mathrm{T}} + \Theta^T\beta A(\Theta)) \\ &\quad - \frac{(1+\cos\theta)(\theta-\sin\theta)}{2\theta\sin^2\theta} S(\Theta)\beta\Theta^{\mathrm{T}} \\ &\quad + \left(\frac{(1+\cos\theta)(\theta+\sin\theta)}{2\theta^3\sin^2\theta} - \frac{2}{\theta^4}\right)\Theta^{\mathrm{T}}\beta\Theta\Theta^{\mathrm{T}}, \\ S(\Theta) &= I + \frac{1-\cos\theta}{\theta^2}\Theta^\times + \frac{\theta-\sin\theta}{\theta^3}\Theta^{\times2}, \\ A(\Theta) &= I + \frac{1}{2}\Theta^\times + \left(\frac{1}{\theta^2} - \frac{1+\cos\theta}{2\theta\sin\theta}\right)(\Theta^\times)^2, \\ \Theta &= \theta\hat{e} = \theta[e_1\ e_2\ e_3]^{\mathrm{T}}, \end{aligned} \tag{7}$$

where θ denotes the principal angle of rotation and $\hat{e} = [e_1\ e_2\ e_3]^{\mathrm{T}} \in \mathbb{S}^2$ is the unit vector along the principal axis of rotation.

The inverse kinematics equation which relates the exponential coordinates and their rates $(X, \dot{X})$ to the vehicle's velocities ξ is given by

$$\xi = G^{-1}(X)\dot{X}, \tag{8}$$

where

$$G^{-1}(X) = \begin{bmatrix} A^{-1}(\Theta) & 0 \\ -A^{-1}(\Theta)T(\Theta,\beta)A^{-1}(\Theta) & A^{-1}(\Theta) \end{bmatrix}$$

and

$$A^{-1}(\Theta) = I + \frac{\cos(\theta)-1}{\theta^2}\Theta^{\times} + \frac{\theta - \sin(\theta)}{\theta^3}(\Theta^{\times})^2.$$

The structure of $G^{-1}(X)$ mentioned here is a direct consequence of the expression for $G(X)$ in eq. (6) and the expression for $A^{-1}(\Theta)$ can be obtained from series expansions stated in [17] or symbolic manipulations.

C. Underactuation Constraint

This paper considers a class of under-actuated vehicles that have actuation for three rotational degrees of freedom (DOF) and one translational DOF, e.g., rotorcraft UAVs with rotors along a fixed plane. In a kinematic model, the vehicle is characterized by the fact that the components of translational velocity ν perpendicular to the vehicle's thrust direction are zero. Let us consider the body-fixed thrust direction to be along the third axis of frame $\mathcal{B}$ represented by the unit vector $\eta = [0 \;\; 0 \;\; 1]^{\mathrm{T}}$. This implies that the translation velocity is of the form

$$\nu = \pm\|\nu\|\eta$$

where $\|\cdot\|$ is the Euclidean norm. Using the inverse kinematics relation in eq. (8), the underactuation constraint for a vehicle considered in this work can be expressed as

$$\pm\|\nu\|\eta = A^{-1}(\Theta)\left(-T(\Theta,\beta)A^{-1}(\Theta)\dot{\Theta} + \dot{\beta}\right). \tag{9}$$

The objective of this paper is to address the problem of generating a trajectory in exponential coordinates (Θ, β) that complies with the underactuation constraint in eq. (9).

III. Trajectory Generation Scheme on SE(3)

This section provides details on the trajectory generation scheme that enables the vehicle to traverse from a given initial pose,

$$g_i = \begin{bmatrix} R_i & b_i \\ 0 & 1 \end{bmatrix},$$

at time t_i to a desired final pose,

$$g_f = \begin{bmatrix} R_f & b_f \\ 0 & 1 \end{bmatrix},$$

at time t_f while simultaneously satisfying the underactuation constraint in eq. (9).

A. Controllability of Underactuated System on SE(3)

The underactuation constraint in eq. (9) can be rephrased as the following control problem

$$\dot{\beta} = T(\Theta,\beta)A^{-1}(\Theta)\dot{\Theta} + A(\Theta)\eta\lambda \tag{10}$$

where $\lambda = \pm||\nu||$ is the magnitude of translational velocity acting as the control input. This is a coupled differential equation in the exponential coordinates Θ and β. Solving eq. (10) is only possible by manipulating the term $T(\Theta,\beta)A^{-1}(\Theta)\dot{\Theta}$, using the expressions in eq. (7), to be

$$T(\Theta,\beta)A^{-1}(\Theta)\dot{\Theta} = U(\Theta,\dot{\Theta})\beta$$

where

$$\begin{aligned} U(\Theta,\dot{\Theta}) = &-\frac{1}{2}\dot{\Theta}^{\times}S \\ &+ \left(\frac{1}{\theta^2} - \frac{1+\cos\theta}{2\theta\sin\theta}\right)(\dot{\Theta}\Theta^{\mathrm{T}} + \Theta\dot{\Theta}^{\mathrm{T}}(A^{-1})^{\mathrm{T}}) \\ &- \frac{(1+\cos\theta)(\theta-\sin\theta)}{2\theta\sin^2\theta}\Theta^{\mathrm{T}}A^{-1}\dot{\Theta}S \\ &+ \left(\frac{(1+\cos\theta)(\theta+\sin\theta)}{2\theta^3\sin^2\theta} - \frac{2}{\theta^4}\right)\Theta\Theta^{\mathrm{T}}A^{-1}\dot{\Theta}\Theta^{\mathrm{T}}. \end{aligned} \tag{11}$$

As a result of this manipulation, it can inferred that if Θ is prescribed as a function of time t, then the constraint equation in eq. (10) is a linear time-varying (LTV) system in β given by

$$\dot{\beta} = U(\Theta(t),\dot{\Theta}(t))\beta + v(t)\lambda \tag{12}$$

where $v(t) = A(\Theta(t))\eta$. As per the assumption on the class of vehicles considered, it is possible to actuate all three rotational DOFs. Hence it is justified to provide the above system with an a priori known or designed function for the exponential coordinate corresponding to attitude i.e. $\Theta(t) : \mathbb{R} \to \mathbb{R}^3$. This work hereafter considers solutions of the form

$$\Theta(t) = \theta(t)\hat{e}$$

where $\hat{e}$ is the constant unit vector relating given initial attitude R_i and final attitude R_f through the equation

$$\exp((\Delta\theta)\hat{e}^{\times}) = R_f R_i^{-1} \tag{13}$$

where $\Delta\theta$ satisfies the relation $\Delta\theta = \theta(t_f) - \theta(t_i)$. With this assumption on $\Theta(t)$, the expression for $U(\Theta,\dot{\Theta})$ simplifies to

$$U(\Theta,\dot{\Theta}) = \frac{\dot{\theta}}{\theta}(I - A(\Theta)) \tag{14}$$

as shown in Appendix VI-A. As the expression for $U(\Theta,\dot{\Theta})$ is considerably simplified, it is easy to assess the controllability of the LTV system. It is well known that a system is controllable if the controllability Gramian defined by

$$W_c(\tau,t_i) = \int_{t_i}^{\tau}\Phi(\tau,\rho)v(\rho)v(\rho)^{\mathrm{T}}\Phi(\tau,\rho)^{\mathrm{T}}\mathrm{d}\rho \tag{15}$$

is positive definite for $\tau \in [t_i, t_f]$. The quantity $\Phi(\tau, t_i)$ is the state transition matrix for the system described in eq. (12) and is given by the matrix exponent

$$\Phi(\tau, t_i) = \exp\left[\int_{t_i}^{\tau} U(\rho)d\rho\right], \tag{16}$$

because $U(t)$ commutes with $U(\tau)$, i.e. $U(t)U(\tau) = U(\tau)U(t)$, for all $t, \tau \in [t_i, t_f]$. In this case, the positive definiteness of $W_c(\tau, t_i)$ can be ascertained by showing that there exists no $q \in \mathbb{R}^3$ such that

$$q^{\mathrm{T}}\Phi(\tau, \rho)v(\rho)v(\rho)^{\mathrm{T}}\Phi(\tau, \rho)^{\mathrm{T}}q = 0, \ \forall\ \rho \in [t_i, \tau]. \tag{17}$$

As $\Phi(\tau, \rho)$ and $v(\rho)$ depend on the choice of $\Theta(t)$, it is shown, in Appendix VI-B, that the system is controllable for all

$$\hat{e} = \{[e_1\ e_2\ e_3]^{\mathrm{T}} : \hat{e} \in \mathbb{S}^2, e_3 \neq \{0, 1\}\}$$

with an underlying assumption that $\theta(t)$ is not constant, i.e., $\theta(t_i) \neq \theta(t_f)$. This assures that the system in eq. (12) is always controllable apart from when the principal axis of rotation $\hat{e}$, relating the initial and final attitudes, is either horizontal (i.e., $\hat{e} = [e_1\ e_2\ 0]^{\mathrm{T}}$) or vertical (i.e., $\hat{e} = [0\ 0\ 1]^{\mathrm{T}}$). Since the controllability of the state $\beta(t)$ is assured and because the intention is to construct a scheme which takes the vehicle to a desired final state β_f we define a difference term $\tilde{\beta}$ as

$$\tilde{\beta}(t) = \beta(t) - \beta_f. \tag{18}$$

The system in eq. (12) can be rewritten in terms of $\tilde{\beta}$ as

$$\dot{\tilde{\beta}} = U(t)\tilde{\beta} + U\beta_f + v(t)\lambda, \tag{19}$$

with an underlying assumption that the vehicle comes to rest at final time t_f, i.e. $\dot{\beta}_f = 0$.

B. Optimal Trajectory Generation for Underactuated System on SE(3)

To optimally solve for $\tilde{\beta}(t)$, the system in eq. (19) has to be slightly altered to get rid of the $U\beta_f$ term. This is done by decomposing λv as a summation of two vectors: one along $U\beta_f$ and the other perpendicular to it, i.e.

$$\begin{aligned} \lambda v &= \bar{\lambda} v_{\beta_f} + kw \text{ where } v_{\beta_f} = (v^{\mathrm{T}}x)x, \\ w &= v - v_{\beta_f} \text{ and } x = \frac{U(t)\beta_f}{||U(t)\beta_f||}. \end{aligned} \tag{20}$$

Setting $\bar{\lambda} = \{-||U(t)\beta_f||/v^{\mathrm{T}}x : v^{\mathrm{T}}x \neq 0\}$ in the above equation results in

$$U\beta_f + \lambda v = kw.$$

Incorporating this into eq. (19) gives the state equation

$$\dot{\tilde{\beta}} = U(t)\tilde{\beta} + w(t)k \tag{21}$$

that can be optimally solved to determine the control input k. Using the standard LQR approach, the optimal trajectory is generated by minimizing the following cost function

$$J = \tilde{\beta}_f^{\mathrm{T}} H \tilde{\beta}_f + \int_{t_i}^{t_f} [\tilde{\beta}(\tau)^{\mathrm{T}} Q \tilde{\beta}(\tau) + rk(\tau)^2]\mathrm{d}\tau, \tag{22}$$

where $\tilde{\beta}_f = \beta(t_f) - \beta_f$; Q, H are positive definite matrices and r is a positive scalar. Minimizing J in (22) results in a control law of the form

$$k(t) = \kappa(t)\tilde{\beta}(t) = -\frac{1}{r}w^{\mathrm{T}}(t)P(t)\tilde{\beta}(t) \tag{23}$$

where $P(t)$ is the solution of the matrix Riccati differential equation (MRDE)

$$\dot{P} + PU + U^{\mathrm{T}}P - \frac{2}{r}Pww^{\mathrm{T}}P + Q = 0 \tag{24}$$

with the boundary condition $P(t_f) = H$. Substituting the control law in eq. (23) into the state equation eq. (21), results in:

$$\dot{\tilde{\beta}}(t) = \left[U(t) - \frac{1}{r}w(t)w^T(t)P(t)\right]\tilde{\beta}(t), \tag{25}$$

which is solved with the initial value of $\tilde{\beta}(t_i) = \beta_i - \beta_f$. Stable convergence of $\tilde{\beta}$ to the zero vector, and therefore of $\beta(t)$ to β_f, follows from the properties of the optimal solution to this LQR problem.

IV. Numerical Simulation

This section presents numerical simulation results of the trajectory generation scheme described in section III. The scheme is generated for a time duration of $t_f - t_i = 10$ s with a time step size of $\Delta t = 0.01$ s. The initial position vector is $b_i = [2\ 1\ 2.5]^{\mathrm{T}}$ and the desired final position vector is $b_f = [1.5\ \ 0.7\ \ 1]^{\mathrm{T}}$. For the purpose of simulating this trajectory generation scheme, it is assumed that the attitude trajectory is prescribed by $\hat{e}$ and θ as follows:

$$\hat{e} = \frac{1}{\sqrt{17}}[2\ \ 2\ \ 3]^{\mathrm{T}}, \text{ and} \tag{26}$$

$$\theta(t) = \frac{3\pi}{5}\sin(0.07\pi t + \frac{2\pi}{3})\ \forall\ t \in [0, 10]. \tag{27}$$

However, if rotation matrices R_i and R_f are provided then $\hat{e}$ can be calculated using eq. (13). Figure 2 shows the time plot of the exponential coordinates $\Theta(t)$ for the attitude. For the cost function J, the quantities Q, r and H are defined to be

$$Q = 500I_{3\times3},\ H = 0_{3\times3},\ r = 100.$$

where $I_{3\times3}$ is the 3×3 identity matrix.

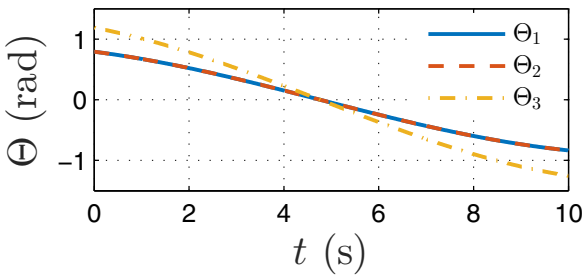

Fig. 2: Time plot of the components of the exponential coordinate vector $\Theta(t)$ corresponding to the generated attitude trajectory.

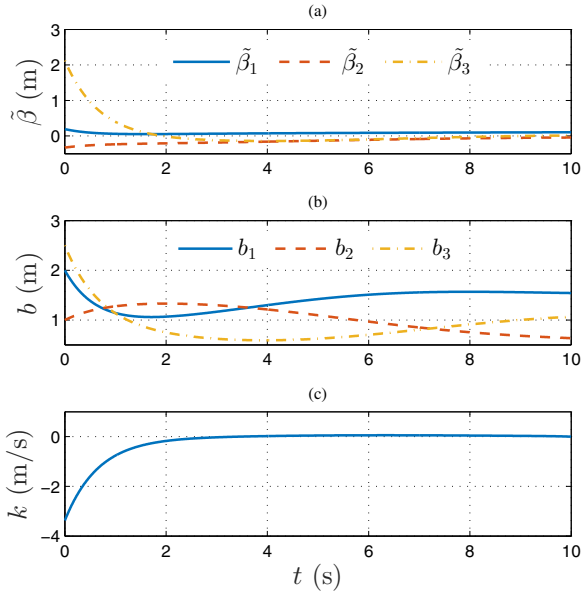

Fig. 3: Simulation results for the position trajectory generation: (a) compoents of $\tilde{\beta}$ converge to zero; (b) components of position vector converge to desired b_f; (c) control input converges to zero.

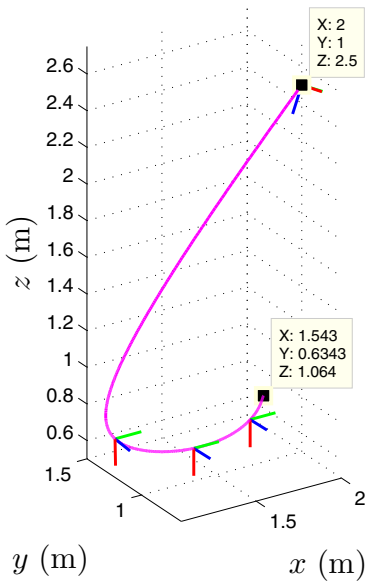

Fig. 4: Trajectory generated for underactuated vehicle on SE(3).

The control law in eq. (23) is calculated by first solving the MRDE backwards in time. This is subsequently used to solve for $\tilde{\beta}$ forwards in time using eq. (25). These differential equations are solved using a fourth order Runge-Kutta method with fixed time step. Simulation results shown in Fig. 3 demonstrate that the quantity $\tilde{\beta}$ asymptotically converges to zero, which is the globally asymptotically stable equilibrium state for the feedback system eq. (25). Further, the position vector $b(t)$ is calculated using the exponential map provided in eq. (4). As a consequence, the convergence of $\tilde{\beta}$ is reflected in Fig. 3 where b reaches the desired final position b_f. Fig. 3 also demonstrates that the control effort $k(t)$ tends to zero asymptotically. This implies that the system reaches its equilibrium, i.e. $\tilde{\beta} = 0$, demonstrating that it is globally asymptotically stable. Once the exponential coordinates $(\Theta(t), \beta(t))$ are known, eq. (4) is employed to determine the pose g of the vehicle. Fig. 4 depicts the generated trajectory of the vehicle traversing from the given initial pose to the desired final pose. Note that this trajectory is smooth and starts and ends with zero velocities.

V. Conclusion

A trajectory generation scheme for an underactuated vehicle modeled as a rigid body is formulated. Of the six degrees of freedom of the rigid body, one translational DOF and all three DOFs of rotational motion are actuated. This scheme generates a trajectory between a given initial pose and a desired final pose using exponential coordinates. The initial and final attitude are related by a rotation about a single principal axis. Generating the trajectory in terms of exponential coordinates is beneficial, as it makes it possible to describe a wide range of motions. The underactuation constraint is also embedded into the trajectory generation problem using exponential coordinates. The time trajectory for the attitude (rotational DOFs) is first prescribed, and the position trajectory is then designed using an LQR approach. Numerical simulation results confirm the performance of this trajectory generation between a given initial pose and desired final pose with zero initial and final velocities and with a single axis rotation. Future work will look at generalizing this trajectory generation scheme to generate smooth trajectories between pairs of initial pose and final pose without restricting to single axis rotations and rest-to-rest maneuvers.

VI. Appendix

A. Simplifying $U(\Theta, \dot{\Theta})$

The quantities used to express $U(\Theta, \dot{\Theta})$ in eq. (11) can be simplified, as follows, by considering $\Theta(t) = \theta(t)\hat{e}$

$$(\Theta^{'})^{\times} S = \theta' \left(\frac{\sin\theta}{\theta} \hat{e}^{\times} + \frac{1-\cos\theta}{\theta} \hat{e}^{\times 2} \right)$$
$$\Theta(\Theta^{'})^{T} (A^{-1})^{T} + \Theta^{'} \Theta^{T} = 2\theta'\theta \left(I + \hat{e}^{\times 2} \right)$$

$$\Theta^{T} A^{-1} \Theta^{'} S = \theta'\theta \left(I + \frac{1-\cos\theta}{\theta} \hat{e}^{\times} + \frac{\theta - \sin\theta}{\theta} \hat{e}^{\times} \right)$$
$$\Theta\Theta^{T} A^{-1}(\Theta) \Theta^{'} \Theta^{T} = \theta'\theta^{3} \left(I + \hat{e}^{\times 2} \right).$$

The resultant expression for $U(\Theta, \dot{\Theta})$ is

$$U(\Theta, \dot{\Theta}) = -\dot{\theta}\left(\frac{1}{2}\hat{e}^{\times} + \left(\frac{1}{\theta} - \frac{1+\cos\theta}{2\sin\theta}\right)\hat{e}^{\times 2}\right)$$
$$= \frac{\dot{\theta}}{\theta}\left(I - A(\Theta)\right),$$

which is identical to eq. (14).

B. Proof of Controllability

The controllability Gramian for the LTV system (12) is defined by

$$W_c(\tau, t_i) := \int_{t_i}^{\tau} \Phi(\tau,\rho)A(\rho)\eta\eta^{\mathrm{T}}A(\rho)^T\Phi(\tau,\rho)^T \mathrm{d}\rho.$$

where $\eta = [0\ 0\ 1]^{\mathrm{T}} \in \mathbb{R}^3$ is the control influence matrix. Evaluating and simplifying the expression (16) for $\Phi(\tau,\rho)$ for $U(\Theta, \dot{\Theta})$ given by eq. (14), gives

$$\Phi(\tau,\rho)A(\rho) = I + w_1(\tau,\rho)\hat{e}^{\times} + w_2(\tau,\rho)\hat{e}^{\times 2},$$

where

$$w_1(t,\rho) = k_1 \sin(\theta(\rho) - \phi),$$
$$w_2(t,\rho) = 1 - k_1\cos(\theta(\rho) - \phi),$$
$$\text{with } k_1 := \frac{\theta(t)}{2\sin\frac{\theta(t)}{2}} \text{ and } \phi := \frac{\theta(t)}{2}.$$

For controllability, it is necessary and sufficient to show that the there exists no non-zero vector $q = [q_1\ q_2\ q_3]^{\mathrm{T}} \in \mathbb{R}^3$ such that [19]

$$Q(\rho) = q^{\mathrm{T}}\Phi(\tau,\rho)A(\rho)\eta = 0, \quad \forall\ \rho \in [t_i, \tau]. \tag{28}$$

(Note that the LTV system (12) is not controllable if and only if there exists $q \in \mathbb{R}^3$, such that $q^{\mathrm{T}}W_c q = \int_{t_i}^{\tau} Q(\rho)^2 \mathrm{d}\rho = 0$.) This condition can be expressed as:

$$Q(\rho) = f(\rho) + e_3\sum_{i=1}^{3} q_i e_i = 0, \tag{29}$$

where

$$f(\rho) = k_1\sin[\theta(\rho) - \phi](q_1e_2 - q_2e_1) -$$
$$k_1\cos[\theta(\rho) - \phi](e_3\sum_{i=1}^{3} q_ie_i - q_3)$$

and $\hat{e} = [e_1\ e_2\ e_3]^{\mathrm{T}} \in \mathbb{S}^2$ is the principal rotation axis corresponding to $R_f R_i^{-1}$. The quantity Q is expressed, in eq. (29), as a sum of function $f(\rho)$ and a constant $e_3\sum_{i=1}^{3} q_ie_i$ for a vector $q \in \mathbb{R}^3$. When $f(\rho) \neq 0$ for all $\rho \in [t_i, \tau]$ then $f(\rho)$ is not of constant value because $\theta(\rho)$ is a time varying quantity. This implies that Q in eq. (29) cannot be zero over the whole interval $\rho \in [t_i, t_f]$. But when $f(\rho) = 0$, i.e., if q is such that

$$q_1e_2 - q_2e_1 = 0, \text{ and}$$
$$e_3\sum_{i=1}^{3} q_ie_i - q_3 = 0, \tag{30}$$

then the following cases arise:

1) If $q = \alpha\hat{e}$ for a constant $\alpha \in \mathbb{R}$, then $Q = \alpha e_3$. When $e_3 = 0$ the system loses controllability.
2) Alternatively, if $e_3 = 1$ then $Q = q_3$; implying loss of controllability when $q_3 = 0$.

This analysis shows that for every

$$\hat{e} = \{[e_1\ e_2\ e_3]^{\mathrm{T}} : \hat{e} \in \mathbb{S}^2, e_3 \notin \{0, 1\}\},$$

the system is controllable.

References

[1] M. Kobilarov, "Trajectory tracking of a class of underactuated systems with external disturbances," in *American Control Conference (ACC), 2013*, 2013, pp. 1044–1049.

[2] D. Mellinger, N. Michael, and V. Kumar, "Trajectory generation and control for precise aggressive maneuvers with quadrotors," *The International Journal of Robotics Research*, vol. 31, no. 5, pp. 664–674, 2012.

[3] T. Lee, M. Leok, and N. H. McClamroch, "Geometric tracking control of a quadrotor UAV on SE(3)," in *49th IEEE Conference on Decision and Control (CDC)*. IEEE, 2010, pp. 5420–5425.

[4] P. Tabuada and P. Lima, "Position tracking for underactuated rigid bodies on SE(3)," ISR Internal Report RT-401-2000, Tech. Rep., 2000.

[5] A. P. Aguiar and J. P. Hespanha, "Position tracking of underactuated vehicles," in *American Control Conference (ACC), 2003*, vol. 3. IEEE, 2003, pp. 1988–1993.

[6] A. Baviskar, M. Feemster, D. Dawson, and B. Xian, "Tracking control of an underactuated unmanned underwater vehicle," in *American Control Conference (ACC), 2005*. IEEE, 2005, pp. 4321–4326.

[7] A. M. Lekkas, "Guidance and path-planning systems for autonomous vehicles," Ph.D. dissertation, Norwegian University of Science and Technology (NTNU), 2014.

[8] N. E. Leonard, "Periodic forcing, dynamics and control of underactuated spacecraft and underwater vehicles," in *34th IEEE Conference on Decision and Control (CDC)*, vol. 4. IEEE, 1995, pp. 3980–3985.

[9] P. Casau, R. G. Sanfelice, R. Cunha, D. Cabecinhas, and C. Silvestre, "Global trajectory tracking for a class of underactuated vehicles," in *American Control Conference (ACC), 2013*. IEEE, 2013, pp. 419–424.

[10] M. Hua, T. Hamel, P. Morin, and C. Samson, "Introduction to feedback control of underactuated VTOL vehicles," *IEEE Control Systems Magazine*, vol. 33, no. 1, pp. 61–75, 2013.

[11] D. Pucci, T. Hamel, P. Morin, and C. Samson, "Nonlinear feedback control of axisymmetric aerial vehicles," *Automatica*, vol. 53, pp. 72–78, 2015.

[12] M. Cutler and J. How, *Actuator Constrained Trajectory Generation and Control for Variable-Pitch Quadrotors*. American Institute of Aeronautics and Astronautics, 2017/03/19 2012. [Online]. Available: http://dx.doi.org/10.2514/6.2012-4777

[13] J. Gillula, H. Huang, M. Vitus, and C. Tomlin, "Design of guaranteed safe maneuvers using reachable sets: Autonomous quadrotor aerobatics in theory and practice," in *IEEE International Conference on Robotics and Automation (ICRA)*, 2010, pp. 1649–1654.

[14] S. P. Viswanathan, A. Sanyal, and M. Izadi, "Integrated guidance and nonlinear feedback control of underactuated unmanned aerial vehicles in SE(3)," in *AIAA Guidance, Navigation, and Control Conference, AIAA SciTech Forum*, no. AIAA 2017-1044, 2017. [Online]. Available: http://dx.doi.org/10.2514/6.2017-1044

[15] S. P. Viswanathan, A. K. Sanyal, and R. Warier, "Finite-time stable tracking control for a class of underactuated aerial vehicles in SE(3)," in *American Control Conference*, Seattle, WA, May 2017, p. to appear.

[16] V. S. Varadarajan, *Lie Groups, Lie Algebras, and Their Representations*. New York: Springer Verlag, 1984.

[17] F. Bullo and R. M. Murray, "Proportional derivative (PD) control on the Euclidean group," California Institute of Technology, Technical Report Caltech/CDS 95–010, May 1995, Available at http://resolver.caltech.edu/CaltechCDSTR:1995.CIT-CDS-95-010.

[18] D. Lee, A. K. Sanyal, E. A. Butcher, and D. J. Scheeres, "Finite-time control for spacecraft body-fixed hovering over an asteroid," *IEEE Transactions on Aerospace and Electronic Systems*, vol. 51, no. 1, pp. 506–520, January 2015.

[19] C. Chen, *Linear System Theory and Design*, ser. Linear System Theory and Design. Oxford University Press, 1999.